Title

The Preparation of Thin Ordered Transition Metal Oxide Films on Metal Single Crystals for Surface Science Studies

Authors

Vurens, G.H.
Salmeron, E.M.
Somorjai, Gabor A.

Publication Date

1990-02-01

LBL-28696
Preprint

Center for Advanced Materials

CAM

Submitted to Progress in Surface Science

The Preparation of Thin Ordered Transition Metal Oxide Films on Metal Single Crystals for Surface Science Studies

G.H. Vurens, M. Salmeron, and G.A. Somorjai

February 1990

Materials and Chemical Sciences Division

Lawrence Berkeley Laboratory • University of California

ONE CYCLOTRON ROAD, BERKELEY, CA 94720 • (415) 486-4755

Prepared for the U.S. Department of Energy under Contract DE-AC03-76SF00098

DISCLAIMER

LBL-28696

The Preparation of thin ordered Transition Metal Oxide Films on Metal Single Crystals for Surface Science Studies

G.H. Vurens, M. Salmeron and G.A. Somorjai

February 23, 1990

Materials and Chemical Sciences Division
Lawrence Berkeley Laboratory
1 Cyclotron Road
Berkeley, CA 94720

This work was supported by the Director, Office of Energy Research, Office of Basic Energy Sciences, Materials Sciences Division, of the U.S. Department of Energy under Contract No. DE-AC0-3-76SF00098.

Abstract

In this paper the preparation, characterization and properties of metal oxide overlayers on dissimilar metal substrates is reviewed. It is shown that using a general recipe metal oxide surfaces can be produced, which are easily accessible with modern surface science techniques. Many different stoichiometries and structures of the oxides can be prepared by variation of the preparation conditions, that do or do not have a counterpart in bulk oxide surfaces. In addition information about the metal oxide surfaces is obtained without experimental problems such as sample mounting, sample heating and sample purity.

Contents

Abbreviations

AES: Auger Electron Spectroscopy

ESCA: Electron Spectroscopy for Chemical Analysis

FEM: Field Emission Microscopy

FIM: Field Ion Microscopy

ISS: Ion Scattering Spectroscopy

LEED: Low Energy Electron Diffraction

MOS: Metal Oxide Semiconductor

SMSI: Strong Metal Support Interaction

STM: Scanning Tunneling Microscopy

TDS: Thermal Desorption Spectroscopy

TPD: Thermal Programmed Desorption

UHV: Ultra High Vacuum

UPS: Ultraviolet Photoelectron Spectroscopy

WF: Work Function

XPS: X-ray Photoelectron Spectroscopy

1 Introduction

The study of metal oxide overlayers on metal substrates is an important field in physics and chemistry. The formation of the metal-oxide interface can be studied with the modern surface science techniques. The growth mode i.e. whether an oxide grows in a three or two dimensional fashion is an important aspect of the interface formation. Also as a result of the oxide substrate interaction an alteration of the chemical properties of the substrate is often observed. The oxide surface formed on top of the metal could be a surface that has no counterpart in its bulk oxide surfaces, both with respect to structure and stoichiometry. Thus oxide surfaces with new properties can be prepared.

Most surface science studies are performed on mono-atomic solids, since it is generally easy to prepare clean and well ordered surfaces of these materials. Many attempts have been made to study the metal oxides in polycrystalline and single crystalline form. Because of their insulating and brittle nature these samples often give rise to experimental problems, such as sample mounting, sample heating and charging problems due to the fact that many surface science techniques utilize charged particles (electrons and ions). In the case of single crystalline oxides it is many times very difficult to prepare samples with other than the basal plane orientation. The electrical and heat conductivities of the oxides are hard to influence without increasing the defect and impurity concentration above an allowable level. Metal oxides often exhibit high solubilities for the for different impurities, such as carbon, sulfur and silicon, that readily segregate to the surface upon heating. In this way the impurities make the investigation of the surface properties of the metal oxide difficult.

One way to solve these problems is by oxidizing a metal substrate, so that a thin film of metal oxide is formed on top of the substrate metal. The electrical and heat conductivity characteristics of the substrate metal eliminate the above mentioned experimental problems. However in this case it is hard to control the stoichiometry and thickness of the oxide layer during subsequent experiments, since the oxygen affinity of the substrate is the same as the oxygen affinity of the metal in the substrate. This means entropy is a strong driving force for the oxygen to diffuse into the substrate and thereby effectively changing the stoichiometry and thickness of the oxide layer. In addition most oxide films are either amorphous or highly disordered. Growth and nucleation of these surface oxide layers, that initiates at defects can give rise to a non-uniform film.

In this paper we present another approach consisting of the deposition of dissimilar metal

oxide overlayers on a metal substrate. In this way the thickness of the oxide can be controlled by the amount of metal oxide deposited on the substrate and the stoichiometry can be controlled by the oxygen dose or the treatment of the sample. Still the advantage exists of having a metal substrate, which is easy to mount and heat and does not have charging problems due to the small thickness of the overlayer (less than 10Å). The oxides formed on top of dissimilar metals will not necessarily have the same structure and stoichiometry as the bulk metal oxides. Since the metal oxide overlayers are thin, a large influence from the substrate and from the interface between the oxide and the metal is expected. These oxides will possibly exhibit different electronic and chemical properties from the substrate metal alone or the oxide alone.

There are many reasons for studying metal oxides on dissimilar metals. In catalysis and in cathodic emission one is interested in the influence of small amounts of metal oxide deposits on the chemical properties of the substrate metal. Also in catalysis one is interested in the catalytic properties and the surface characteristics of the metal oxides themselves. The Metal Oxide Semiconductor (MOS) technology is interested in the electrical conductivity and the interfacial properties of the oxides. Still another reason for the interest in metal oxides lies in the study of the oxidation characteristics of the overlayer metal, in order to get a fundamental understanding of the oxidation processes.

Many studies have appeared on the alkali and alkaline earth metal oxide overlayers on dissimilar substrate metals. These overlayers have applications in low work function electron emitters. This paper summarizes the studies performed by deposition of monolayer and submonolayer amounts of transition metal oxides on dissimilar metal substrates. It discusses the different methods of preparation, the characterization techniques, the different chemical and electronic properties and the different structure and stoichiometries of these oxide overlayers.

2 Preparation of Metal Oxide Overlayers

There are about as many different ways of preparing the transition metal overlayers as there are papers published on this subject. Therefore it is impossible to give a general recipe on how exactly to prepare these overlayers, but the following description covers most of the preparation procedures and is shown schematically in figure 1.

Metal oxides can generally be grown on metal substrates using a three step process.

I) Evaporation of the metal onto the substrate. The metal evaporation can be done with any type of metal evaporation source. Metal evaporators that have been used are metal filaments

made out of the transition metal to be evaporated or made out of transition metal- refractory metal alloys. Most common is the mixed metal filament, in which a wire of the metal to be evaporated is wrapped around a refractory metal wire that is heated either resistively or by electron bombardment. Other ways to evaporate the metals such as Knudsen cells and argon sputtering of the transition metal onto the sample have been used.

II) Oxidation of the metal with oxygen. The oxygen pressures used range from 5×10^{-8} Torr to 760 Torr.

III) Heating of the substrate to temperatures ranging from 300 - 1300 K is necessary to produce ordered oxide films

IV) In the study of small amounts of oxide, where a fraction of the substrate metal is still exposed to the vacuum, it may be necessary to selectively remove oxygen from the uncovered substrate metal by a suitable titration. The heating of the substrate can be carried out in the presence of oxygen, effectively combining steps II and III. It is also possible to combine all three steps, i.e. evaporate the transition metal in the presence of oxygen onto a heated substrate. Depending on the chemical properties of the substrate metal, it might be necessary to add reducing treatments.

Rarely oxide sources are used to prepare metal oxide overlayers. The metal oxide is heated in a refractory metal boat or it is pasted on a refractory metal filament that is heated. This usually results in the formation of a rather reduced metal oxide overlayer [1-8].

The deposition of zinc oxide films, has been problematic from an experimental point of view. Zinc metal has a high vapor pressure at relatively low temperatures and therefore it is incompatible with the surface science ultra high vacuum (UHV) equipment used in the characterization and study of these films. If the metal is to be deposited the evaporation source has to be cooled down during bake out of the vacuum system. If such care is not taken unwanted deposition of the zinc oxide can occur over the whole vacuum chamber [9]. Zinc oxide can also be deposited by evaporation of liquid droplets saturated with ZnO [10]. However in this way it is difficult to control the thickness of the metal oxide overlayer.

3 Stoichiometry of metal oxide overlayers

Most metal oxides that are in the solid state under atmospheric conditions at room temperature are also stable under ultra high vacuum conditions at room temperature. However if the oxide is heated a substantial oxygen pressure may result and the oxide decomposes. Table 1 lists the temperatures at which an oxygen partial pressure of 1×10^{-9} Torr is ex-

pected due to the reaction $M_yO_x = yM + \frac{x}{2}O_2$ for the different metal oxides (see appendix I). A substantial oxygen partial pressure can be obtained at lower temperatures than the ones listed in table 1 due to the decomposition of the metal oxide in suboxides and oxygen. From table 1 it is clear that generally the lowest oxidation state of the metal is most stable. Due to the heating treatments necessary for ordering or oxidizing the metal oxide oftentimes substoichiometric oxides are obtained.

The stoichiometry can to some extent be controlled by the preparation conditions of the oxide. This section reports on the different oxidation states and stoichiometries within oxide overlayers, that have been reported. Table 2 lists the stoichiometries of these oxides. Aluminum oxide if evaporated from an oxide source forms a substoichiometric oxide on polycrystalline tungsten [3, 5, 6, 11], tungsten(112) [3, 4] and rhenium [7]. If aluminum metal is evaporated followed by oxidation of the aluminum metal Al_2O_3 is obtained on rhodium [22-24], iron(100),iron(110),iron(111) [31-33] and platinum [18]. Similarly stoichiometric oxides with the metal in the highest oxidation state like Nb_2O_5 [18, 19, 20], ZrO_2 [21, 22] and SiO_2 [18] were prepared by evaporation of the metal followed by oxidation.

In the case of silicon oxide also SiO could be obtained by using an annealing treatment [18] or by evaporation from an oxide source [1, 2]. Like silicon oxide titanium oxide can be prepared with several different stoichiometries depending on the preparation conditions. On platinum [11-19], rhodium [15,17,20-24] and ruthenium(0001) [32] titanium dioxide is formed with titanium in the Ti^{4+} oxidation state at lower temperatures. Annealing results in the formation of TiO with titanium in the Ti^{3+} oxidation state. On a gold substrate only low temperature deposition of titanium oxide has been reported [13] which resulted in the formation of TiO_2, and on a palladium substrate [27, 19] the stoichiometry is determined to be TiO after an annealing treatment.

Other stoichiometric metal oxide overlayers that have been prepared include PbO on silver [33, 34] and copper [34-37], ZnO on copper [10] and FeO on platinum(111) [38]. Both the lead and iron oxide overlayers are formed with the metal in a lower than its maximum oxidation state. On many occasions a substoichiometric oxide is formed as in the case of manganese oxide on nickel(111) [8], titanium oxide on nickel(111) [39] and neodymium oxide on copper(100) [40].

In most studies the oxide overlayer is a well separated phase from the metal substrate. Only one study [21, 22] reports the formation of a ternary ($PtZr_xO_y$) phase. Obviously in the case of overlayers there is a strong interaction between the overlayer and the substrate

and the phase separation is not always clear. This interaction plays an important role in the stability, growth, structure and properties of the oxides and will be discussed in the subsequent sections.

4 Stability of metal oxide overlayers

Due to the low surface free energy of oxides as compared to metals [41], it is expected that the oxide overlayers on metals are stable up to high temperatures in vacuum conditions, although changes in stoichiometry have to be expected. Upon annealing a metal oxide overlayer can decompose in the metal (or a suboxide) and oxygen, but also the metal oxide can evaporate into the vacuum. A third possible cause for the instability is the diffusion of the metal oxide into the bulk of the substrate metal.

4.1 Decomposition of metal oxide overlayers

An example of the first destabilizing effect, i.e. the case of the oxide is the decomposition of titanium dioxide on palladium which decomposes at 1100 K to form a Pd-Ti alloy [27, 19]. The decomposition of the metal oxide into the metal and oxygen appears to be of little importance in most cases.

4.2 Evaporation of metal oxide overlayers

On refractory metals oftentimes the metal oxide overlayer will evaporate leaving a clean substrate behind. An example is aluminum oxide on tungsten. Aluminum oxide is very stable on tungsten surfaces, as can be derived from the activation energies for desorption from the different tungsten planes [3]. The energies were 79, 95 and 104 kcal/mol for the W(110), W(112) and W(100) respectively. Alumina also completely desorbs from rhenium at about 1600 K [7]. Other metal oxide overlayers such as silicon oxide and chromium oxide will also evaporate from the refractory metal surfaces. Silicon oxide on platinum decomposes at temperatures above 1250 K. Silicon oxide on rhenium starts to desorb slowly at 1340 K [2]. The activation energy for desorption is 3.1 eV (71 kcal/mol), which is very close to the sublimation energy of silicon monoxide. The same 3.1 eV activation energy is found for silicon oxide on tungsten [1]. The stability of the chromium oxide on W(110) was studied by Shinn and Berlowitz [42] with TDS. At chromium oxide coverages below a monolayer a TDS peak at 1370 K on mass 52 is observed. This peak is attributed to the W-Cr interfacial oxide. Patches of Cr_2O_3 desorb at 1500 K. At coverages above a monolayer a multilayer peak

at 1230 K appears. So the stability of chromium oxide on W(110) increases from multilayer CrO_x to monolayer CrO_x to monolayer Cr_2O_3.

4.3 Diffusion of metal oxide overlayers

The diffusion into the substrate is the most important limit to the stability of metal oxide overlayer on non refractory metals. It has been shown [12,17-19] that titanium oxide diffuses into the bulk of platinum at temperatures between 700 - 900 K and reversibly segregates to the surface upon cooling below 500 K. Niobium oxide shows the same behaviour as titanium oxide [18]. Although the segregation did not occur if the niobia was prereduced by electron bombardment before heating. The dissolution of the titanium oxide did not occur on rhodium [27, 19]. Badyal et al. [32] shows that a critical coverage of 0.68 ML of titanium oxide on ruthenium(0001) exists, above which the titanium oxide diffuses into the bulk upon annealing. Zirconium oxide dissolves into a platinum substrate [21] upon annealing above 900 K with complete disappearance of the zirconium from the surface. Exposure to oxygen at room temperature caused the formation of a $PtZr_xO_y$ phase which was stable in oxygen up to 573 K. Iron oxide on platinum(111) is stable until 1050 K when the dissolution of the oxide into the platinum takes place [38]. Neodymium oxide can dissolve in copper(100) upon annealing to temperatures above 800 K [40].

It is clear that the stability of the oxide overlayers on metal substrates is not as much a function of the metal oxide properties, but rather a function of the substrate properties. Off course the properties of the oxide and the substrate can not be separated completely, but that gives rise to the unique properties of the metal oxide overlayers.

5 Nucleation and Growth of metal oxide overlayers

The first step in the characterization of metal oxide overlayers usually is the determination of the nucleation and growth mechanism of the layer. X-ray Photoelectron Spectroscopy (XPS) or Electron Spectroscopy for Chemical Analysis (ESCA) and Auger Electron Spectroscopy (AES) are commonly used to study the growth of the metal oxide overlayer by means of an uptake curve measurement. In these measurements the intensity of one of the substrate peaks in AES or XPS is followed as a function of deposition time. Alternatively the intensity of the adsorbate peaks can also be followed. As long as the adsorbate grows within one atomic layer the intensity of the substrate peak will decrease linearly. However if the deposition of the adsorbate occurs in several atomic layers at the same time a gradual non linear decay in

the substrate intensity in AES or XPS is observed.

If the first atomic layer is completed before the formation of the second atomic layer is started then the attenuation due to the second atomic layer will be less than the attenuation by the first atomic layer. So if the formation of the first atomic layer is finished before the formation of the second atomic layer is started there is a break in the curve of substrate intensity versus deposition time. See figure 2a for an example. In practise it can be difficult to detect such a break due to the fact that in many cases a layer is not totally completed, before the formation of the next layer is started. Also noise in the experiments can contribute to problems in the interpretation of these uptake curves. Figure 2b shows such an uptake curve. Therefore other techniques are necessary to aid in the interpretation.

Ion Scattering Spectroscopy (ISS) and the titration of the surface with a reactive gas are two techniques commonly used to determine the growth mode of an adsorbate in the first atomic layer. ISS that uses low energy (< 1000eV) helium ions is a highly surface sensitive technique that only contains information about the outermost atomic layer. A linear decay of the substrate intensity to zero indicates that the first atomic layer grows in a two dimensional fashion, while if large amounts of adsorbate are necessary to make the substrate intensity disappear then the first and following layers will have grown in a three dimensional fashion. Similar information can be obtained by the titration of the surface with a reactive gas. The area of exposed substrate metal can oftentimes be titrated by adsorbing a saturation dose of a reactive gas (such as CO or H_2). The Thermal Programmed Desorption (TPD) spectrum will then reveal the amount of reactive gas adsorbed on the sample. If the reactive gas only has interaction with the substrate metal and not with the adsorbate under ultra high vacuum conditions, then the area of exposed substrate can be determined. Like ISS this will show if the first atomic layer grows in a two or three dimensional fashion.

Similar to metal on metal overlayers [43] oxides can show the three main modes of growth, Volmer-Weber (growth of three dimensional crystallites of the adsorbate on the substrate surface), Frank-van der Merwe (layer by layer growth of the adsorbate on the substrate) and Stranski-Krastanov (formation of one or more complete monolayer, before the three dimensional crystallite growth is started). Due to the very nature of the oxide overlayer formation, which often involves heating of the substrate, a fourth growth mechanism is likely to appear. It is the surface compound formation, where the substrate and adsorbate metal atoms are mixed in the same layer and perhaps form a mixed oxide. The details of how XPS and AES are used to distinguish between the different growth mechanisms is the

subject of a paper by van Delft et al. [44]. Table 2 lists the growth modes of the different oxides on the substrates.

5.1 Layer by layer growth of metal oxide overlayers

Vurens et. al. [38] uses a combination of techniques in order to determine the growth mode of iron oxide on platinum. AES uptake curves (fig. 2b) are measured as well as CO titration of the substrate. This process uses the fact that under Ultra High Vacuum (UHV) conditions CO only sticks to the platinum and not to the iron oxide overlayer. The disappearance of the CO in the TPD spectra is therefore an indication of the completion of a monolayer. Similarly ISS was used to obtain the monolayer coverage. It should be noted that titration and ISS do not give actual growth mode information, but they provide an excellent way to study when the overlayer completely covers the substrate. Another tool in the layer growth determination is a measurement of the crystal current. This measurement shows a break at the monolayer coverage in many cases. The reason for this break is related to the change in work function of the sample upon oxide deposition and is described in more detail in [38]. A layer by layer growth of the iron oxide on platinum (111) is concluded based on this method. A similar combination of AES uptake curves and CO titration has been used by Badyal et. al. [32] in the study of titanium oxide on ruthenium (0001). It shows that titanium oxide grows in a layer by layer mode. From AES uptake curves and CO titration Levin et al. [14] shows that aluminum oxide on rhodium grows one complete monolayer, before the formation of three dimensional crystallites is started. A Stranski-Krastanov growth mode is also found with titanium oxide on rhodium [31]. Recently Williams et al. [45] showed that titanium oxide grows in a layer by layer fashion on rhodium(111). Bukaluk et al. [9] utilized the AES uptake curve to conclude that the growth of zinc oxide on gold is layer by layer. Bardi et al. reported a layer by layer growth of zirconium oxide on platinum (100).

5.2 Three dimensional growth of metal oxide overlayers

Few oxides actually give a three dimensional growth mode on metal substrates. Ko and Gorte [18] reported that aluminum oxide and silicon oxide show a three dimensional crystallite growth on platinum, after study of the CO chemisorption behaviour of the substrate. Similarly Raupp and Dumesic [46] show that aluminum oxide has a lower dispersion than titanium oxide on nickel, indicating a three dimensional growth of the aluminum oxide. Aluminum oxide also shows a three dimensional growth on iron (111), iron(100) and iron (110)

according to Strongin et al. [16]

5.3 Stranski-Krastanov growth of metal oxide overlayers

Two dimensional growth for the first monolayer is found for many systems. These systems include: titanium oxide on platinum [11-19], titanium oxide on nickel [46, 47], titanium oxide on palladium [27, 19], niobium oxide on platinum [18, 19, 20], silicon oxide on tungsten [1] and manganese oxide on nickel (111) [8]. The investigation of the sub monolayer growth behaviour of the systems was performed with ISS or titration techniques. These systems must either grow with a Frank- van der Merwe layer by layer growth mechanism or grow with a Stranski- Krastanov mechanism. A Volmer-Weber mechanism can be excluded.
Besides the growth mechanism early studies determined the nucleation behaviour of metal oxides on metal substrates using Field Emission Microscopy (FEM). Most often the formation of the oxide growth was started on the vicinal areas of a plane, i.e. on the steps occuring on these planes. Silicon oxide on rhenium [2] nucleates at the vicinal areas of the $(10\bar{1}1)$, $(10\bar{1}0)$, $(11\bar{2}0)$ and $(11\bar{2}2)$ planes. Aluminum oxide on rhenium [7] nucleates at the steps of the $(10\bar{1}1)$ planes. The nucleation of the aluminum oxide on tungsten [3, 4] takes place in the vicinal (stepped planes) areas of the W(110) and (100) planes. However the nucleation on the W(211) plane does not take place at the steps, but immediately on the plane.
Summarizing the above results, we can conclude that most metal oxides wet the surface of metals at least up to one monolayer coverage. Aluminum and silicon oxide generally do not wet the metal surface, with the exception of aluminum oxide on rhodium. There seems to be a correlation between the growth mode of the first atomic layer and the ability of the oxide to form substoichiometric oxides or oxide with the metal in a different valence state. The surface free energy of a metal is substantially reduced by the introduction of oxygen into the system [41, 48]. However the lower the oxygen partial pressure above the oxide, the higher the surface free energy becomes [49, 50]. Therefore the surface free energy is not necessarily minimized at the highest oxygen content of the system, but also depends on the thermodynamic stability of the oxide in ultra high vacuum. The result is that many of the oxides formed in vacuum are substoichiometric. Since not all the metal bonds in a substoichiometric oxide are saturated with oxygen, the metal will form bonds with the substrate. This strong interaction between the oxide overlayer and the substrate gives rise to a two-dimensional growth of the oxide. If a stoichiometric oxide overlayer is formed a three-dimensional growth is expected.

6 Structure of metal oxide overlayers

The geometrical structure of the metal oxide overlayer can be studied by means of Low Energy Electron Diffraction (LEED). LEED will provide the symmetry and size of the unit cell if the oxide overlayer shows long range ordering. No definite information about the relative positions of the atoms within the unit cell can be obtained, without a comparison between theoretical and experimental intensity-voltage curves [51]. These calculations involving multiple scattering theory have not been performed for any transition metal overlayer. It is possible however to obtain more information about the structure of the unit cell by combining LEED information with information from other surface sensitive techniques such as XPS, AES and Ion Scattering Spectroscopy (ISS).

6.1 Zirconium oxide on platinum(100)

Very little is known about the actual structure of oxide overlayers on dissimilar metals. Since LEED is the primary source of information about the oxide structure and thus only oxides deposited on metal single crystals can be studied. Bardi et al. [21, 22] studied the structure of zirconium oxide overlayers on platinum (100). Four different structures of the overlayer oxide were observed. First there is a (100)- (1×1) structure, interpreted as being ZrO_2 islands on top of a Pt(100)-(1×1) surface. The second structure

$$\begin{bmatrix} 2 & 1 \\ \overline{1} & 1 \end{bmatrix}$$

was interpreted as a structure in which Zr^{4+} penetrated the platinum, but the zirconium still had oxygen ligands. The matrix

$$\begin{bmatrix} m_1 & m_2 \\ m_3 & m_4 \end{bmatrix}$$

indicates the components of the new unit cell vectors in terms of the old substrate unit cell vectors. The description of the surface structure with the matrix notation can be found in more detail elsewhere [52]. The

$$\begin{bmatrix} 7 & 0 \\ 0 & 4/3 \end{bmatrix}$$

structure was similar to the

$$\begin{bmatrix} 2 & 1 \\ \overline{1} & 1 \end{bmatrix}$$

structure, but had a lower oxygen content. A fourth rhombic structure was observed

$$\begin{bmatrix} 0.77 & 0.77 \\ \overline{0.57} & 0.92 \end{bmatrix}$$

This structure can be derived from a Zr(0001) hexagonal plane by enlarging the angle and shortening the Zr-Zr distance. From this study it is clear that many different overlayer oxide structures can be prepared on the same substrate by varying the preparation conditions of the oxide.

6.2 Neodymium oxide on copper(100)

A study of the structure of neodymium overlayers on copper (100) was performed by Nix et al. [40]. the structure of these overlayers was studied as a function of annealing temperature in oxygen and as a function of neodymium coverage. Annealing below 550 K in oxygen did not result in an ordered LEED pattern. Several orientations and with various amounts of rotational disorder in the neodymium overlayers were observed as a function of neodymium coverage. Again it is shown that the structure of the oxide is very much dependent on the preparation conditions.

6.3 Titanium oxide on ruthenium(0001)

In the former two cases the direction of the unit cell vectors of the oxide overlayer was not the same as the direction of the unit cell vectors in the substrate. In some cases the directionality of the unit cell vectors is conserved, although the length of the unit cell vectors in the overlayer can vary from the length of the unit cell vectors in the substrate. A perfect (1×1) pattern was obtained for one monolayer coverage of titanium oxide on ruthenium (0001) [32].

6.4 Iron oxide on platinum(111)

An expansion of the unit cell appears in one monolayer of iron oxide on platinum (111) [38]. In this case an expanded "2×2" structure was found at coverages higher than one monolayer. Vurens et al. [38] reports that 6 by 6 iron oxide units cell cover a 7 by 7 platinum unit cell area.

The very limited amount of information available about the structure of these metal oxide overlayers is in many cases complemented by ISS data. In all cases both the metal in the oxide overlayer and oxygen are observed in the ISS spectra, indicating that both the metal and the oxygen are exposed to the vacuum. More structural information cannot be obtained from the published data due to unknown incident and scattering angles and unknown neutralisation cross sections of the rare gases used in ISS.

The fact that oxide overlayers can be ordered often means that these oxide overlayers are strained in order to have epitaxial relationships with the surface. Just as with the growth mode of the oxide, the stoichiometry and therefore the degree of saturation of the bonds is very important. A different stoichiometry leaves a different number of bonds in the oxide overlayer unsaturated. In order to form more or less bonds with the substrate different epitaxial relationships are observed. The epitaxial relationship that is finally observed is determined by minimalization of the energy of the surface. This means the number of bonds of the overlayer with the substrate (and therefore the stoichiometry) and the strain in the overlayer have to be balanced.

7 Electronic Properties of metal oxide overlayers

Early papers dealing with metal oxide overlayers used Field Electron Microscopy (FEM) and Field Ion Microscopy (FIM) to study the nucleation, growth and structure of the oxide overlayers on the different lattice planes exposed at the tips. FEM and FIM also gave insight in the electronic properties of the different oxide covered surfaces.

Work Function (WF) measurements and Ultra violet Photoelectron Spectroscopy (UPS) are routinely used in order to obtain information about the electronic properties, such as the band structure, of these oxide overlayers. Nowadays Scanning Tunneling Spectroscopy (STM) could provide a good insight in the nucleation and growth mechanisms of the oxide as well as additional information about their structure and electronic properties. The STM could also be utilized to study the defect properties of the oxide layer. Although no STM studies of metal oxide overlayers have been reported yet, it is expected that a large number of studies involving this technique will soon appear.

In many of the early studies [2,4-7] Fowler-Nordheim plots were used in order to determine the work function changes on the different planes as a function of oxide coverage. Pankow and Drechsler [11] used the changes in brightness of the screen to study work-function changes of aluminum oxide on tungsten, molybdenum, tantalum and iridium. They also studied the brightness of the screen when gallium, beryllium, magnesium and germanium oxide were deposited on tungsten. Pankow and Drechsler concluded that the geometric properties such as atomic radii are important in the adsorption characteristics of metal oxide systems on metals. Beach and Vanselow [7] also studied the brightness of the screen when aluminum oxide was deposited on rhenium. The high electron emission in the vicinal areas of the $(10\bar{1}1)$ plane was explained by the fact that aluminum was present in the outermost atomic layer.

Nix et al. [40] used UPS to study the oxygen uptake of neodymium overlayers to form neodymium oxide. The addition of oxygen to the neodymium copper system causes a whole range of changes in the atomic positions and work function of the system, depending on the oxygen exposure, neodymium coverage and thermal history of the sample.
Apart from the work by Nix et al. and the studies on the effect of oxide overlayers on the work function, no studies have been made of the band structure with photoemission techniques. Ultra Violet Photoelectron spectroscopy studies of these overlayers can give information about the development of the band structure of the oxide as a function of thickness and stoichiometry. In that way the formation of a band gap in thick oxides and the influence of edge effects in the submonolayer regime can be studied.

8 Chemical Properties of metal oxide overlayers

The defect properties, such as steps and vacancies and chemical properties, such as stoichiometry of the oxide and oxidation state of the metal in the oxide, are commonly studied by the combination of many modern surface science techniques. In particular Thermal Desorption Spectroscopy (TDS) (also known as Temperature Programmed Desorption (TPD)), XPS, AES and ISS. Most studies that have been reported concentrate on the influence of the metal oxide overlayer on the chemical properties of the substrate. High pressure chemical reaction such as CO methanation and ammonia synthesis have been used to study this influence.
The chemical properties of a metal oxide overlayer can roughly be divided in properties of the oxide itself, properties of the substrate and the properties of the metal oxide-substrate interface. Often it is hard to distinguish between the origins of chemical properties. This difficulty is well illustrated by the extensive work studying the Strong Metal Support Interaction (SMSI) phenomena of titanium oxide on several group VIII metals. The SMSI effect is the fact that the activity of metal particles in some catalytic reactions is enhanced by certain metal oxide carriers. Metal oxides that do show this activity enhancement are titania and niobia, while alumina ans silica do not show this activity enhancement.

8.1 Titanium Oxide Overlayers

Raupp and Dumesic [46] in their study of titanium and aluminum oxide on nickel find a maximum decrease of 6 kJ/mol in the CO binding energy upon adsorption on a 10%

titanium covered surface. It is concluded that most effects on the chemisorption behaviour of CO are caused by short range chemical effects.

Dwyer et al. [26] show that the shift of the O-1s and the Ti-2p core levels upon reduction of a titanium oxide overlayer on platinum can be explained by a rearrangement of the electronic structure of the titania metal interface. Upon reduction by CO of the titanium oxide an Ohmic contact is made between the oxide and the metal. However in spite of this change in the interfacial electronic structure no influence can be observed in the CO and H_2 TPD spectra, leading the authors to believe that titanium oxide is a simple site blocker. Similar shifts in the binding energies of the titanium and oxygen peaks are found by Levin et al. [13] for titanium oxide on rhodium. A shift in the opposite direction was observed by Greenlief et al. [29] after annealing titanium oxide on platinum. In this case the shift was explained by an increased final state screening of the O-1s core holes. A shift in the Pt-$4f_{7/2}$ peak to higher binding energy was interpreted as being caused by the Ti-Pt interactions.

Titanium oxide on platinum does not have any influence on the chemisorptive behaviour of H_2 and CO on platinum, except for the blocking of the platinum surface [25]. In contrast to the chemisorption behaviour observed in UHV, TiO_x overlayers have a large influence on chemical reactions like methanation ($CO + H_2 = CH_4$) at atmospheric pressures. Demmin et al. [25, 19] reported in the study of titanium oxide on platinum that although the platinum is completely covered with titanium oxide and the H_2 and CO adsorption is completely suppressed, the methanation reaction still occurs. The reaction did leave carbon behind on the titania covered surface, but no impurities were observed on the clean surface after reaction. The activation energy for the methanation reaction decreased from 30.2 to 18.9 kcal/mol by going from clean platinum to a titanium covered surface. Also the titania covered surface had a higher activity than the clean surface. A difference in reaction order of CO depending on the CO pressure was also observed between the clean and oxide covered surfaces [23].

It was found that [27, 19] that titanium oxide on rhodium also prevented the adsorption of CO and H_2 linearly with coverage. The linear decrease can be explained by the physical blocking of the adsorption sites by the titanium oxide. Levin et al. [31] finds a more substantial decrease in the CO adsorption as titanium oxide would cause by means of site blocking. It was shown that reduction in hydrogen would decrease the adsorption of CO even more. The reduction of the total amount of CO desorbed was increased with higher H_2 reduction temperatures. The apparent disagreement in the adsorption behaviour of CO

as a function of titanium oxide coverage was recently elucidated by Williams et al [45], who concluded that titania on rhodium acts as a simple site blocker for CO adsorption and that Levin et al. used an erroneous coverage calibration.

Levin et al. [30, 12] found a three fold increase in the CO hydrogenation activity over rhodium at a titanium coverage of 0.15 ML (i.e. 0.5 ML after correction). Titania increased the selectivity towards olefin production, while lowering the activation energy from 24.4 to 16.8 kcal/mol. Also both the CO and H_2 reaction order were increased. The results are explained by a model in which Ti^{3+} participates in the dissociation of CO. XPS studies as a function of TiO_x coverage indicated that Ti^{3+} is positioned preferentially at the perimeter of the oxide islands [12, 14].

Palladium is similar to the platinum and rhodium substrates with respect to the chemisorption of CO and H_2 as a function of titanium oxide coverage. [27, 19] Titanium oxide acts like a site blocker in the chemisorption.

Chung et al. [39] shows that the methanation activity of Ni(111) optimizes at 8% of a monolayer coverage of titania. The activity and product distributions are similar to $Ni/TiO_2(100)$. The SMSI effect is explained by the movement of titania to the surface of the nickel metal.

Raupp and Dumesic [46, 47] show that the CO chemisorption strength is significantly weakened by titania species on the nickel surface. CO has two different binding states on the nickel surface. The sticking coefficient of CO decreased from 1 on the clean surface to 0.2 on the titania covered surface. CO adsorbed in the molecular form did not dissociate. H_2 however did dissociate and 3 hydrogen binding states are observed. All these characteristics are observed for SMSI systems. Again it was concluded that the SMSI effect was caused by the movement of the titania onto the surface of the nickel metal.

Badyal et al. [32] showed a different chemisorptive behaviour for CO depending on the pretreatment of the titania overlayer on ruthenium (0001). If the titanium oxide is not annealed, the titania just acts as a site blocker in the chemisorption of CO. If the titania is preannealed however two effects appear. One is the shift towards higher temperature of the CO desorption and the other is the decrease in chemisorption capability more than expected for simple site blocking. Both effects are attributed to electronic effects.

In summary most studies agree on the fact that titanium oxide is a simple site blocker for the chemisorption of CO and H_2 under ultra high vacuum conditions. The reason for its different behaviour under high pressure conditions could be due to weak CO and H_2 binding sites near the oxide metal interface or due to a modification of the oxide structure under

high CO and H_2 pressures.

8.2 Aluminum Oxide Overlayers

Aluminum oxide has also been studied extensively in order to compare its behaviour with that of titania, which is commonly associated with the SMSI effect. Raupp and Dumesic [46] found for aluminum oxide on nickel, that the alumina blocks some adsorption sites for CO and also created some new adsorption sites. The activation energy for desorption was slightly decreased by the alumina. The initial sticking coefficient of the CO remained nearly uninfluenced by the alumina. Alumina blocks the most strongly bound β_1 hydrogen sites, while creating a new even stronger binding site. It is concluded that the effects of aluminum and titanium oxides on the chemisorption properties of metal surfaces, is similar.

Ko and Gorte [18] do not find a change in the chemisorption behaviour of CO and H_2 when aluminum oxide is deposited on platinum. On rhodium it was observed by Levin et al. [12, 14] that aluminum oxide had a site blocking effect on the CO hydrogenation rate of the rhodium. The product distribution and the kinetic parameters of the reaction were unaffected by the presence of the alumina. CO chemisorption is also suppressed in direct proportion to the alumina coverage [14], without affecting the desorption energy.

Strongin et al. shows that the presence of aluminum oxide on the surface of iron stabilizes a reconstruction of the surface that occurs after heating the surface in 20 Torr of water vapor [16, 17]. The authors propose that this reconstruction exposes the planes of iron, that are known to be highly active in ammonia synthesis: Fe(111) and Fe(211). It is also shown that the presence of alumina increases the stability of potassium on the surface during ammonia synthesis [15]. Similar to aluminum oxide, silicon oxide shows no change in the CO chemisorption and desorption behaviour, when deposited on platinum [18].

8.3 Other Metal Oxide Overlayers

Zirconium oxide on platinum(100) [22] showed a site blocking effect upon CO chemisorption. No new CO adsorption states were observed and the blocking occurred linearly with coverage. It is found by Ko and Gorte [18] that the H_2 and CO chemisorption decrease linearly with niobia coverage. Demmin et al. [19] show that the platinum is still active in the methanation reaction even though no CO or H_2 chemisorption is observed. The activation energy for the methanation reaction is 18.7 kcal/mol [20].

Vurens et al. [38] find that CO on platinum(111) desorbs at a lower temperature upon iron

oxide evaporation. This shift is attributed to the fact that more CO occupies a smaller area. Due to the dipole-dipole interactions the desorption peak shifts to lower temperature. At one monolayer coverage the iron oxide blocks the CO adsorption. The water TPD from iron oxide on platinum(111) was also studied. Water has three possible adsorption states on iron oxide, depending on the coverage and the thermal history of the overlayer. The water- oxide interaction differences are attributed to atomic steps and Oxygen vacancies in the oxide.
Zhao et al. [8] in a study of manganese oxide on nickel(111) show that CO chemisorption is suppressed almost linearly with Manganese oxide coverage, indicating a site blocking effect. An additional CO adsorption state at 305 K was found, which was attributed to CO adsorbed on the manganese oxide perimeter. Campbell et al. [10] attempted to activate a Cu(111) single crystal for methanol formation by depositing zinc oxide on the surface. However no measurable activity was found after the ZnO deposition.
The process of the oxidation of the overlayer metal has been the subject of study in many papers. Most of the effort in understanding this oxidation of metal overlayers to form metal oxide overlayers has been focussed on lead overlayers. Chadwick and Christie [35] show that there is a different oxidation behaviour below and above 0.5 ML lead coverage on copper. It is attributed [36] to the spillover of oxygen from the copper. This spillover effect has been confirmed by Ocal et al. [37]. Chadwick and Karolewski [34] found a similar behaviour in the oxidation of lead overlayers on silver. The oxygen sticking coefficient is much higher below 0.5 ML lead coverage, resulting in fast oxidation of the lead, while the sticking coefficient of oxygen above 0.5 ML is much lower. The sudden decrease in the oxidation rate of lead at coverages between 0.5 and 0.7 ML [33] let the authors to the conclusion that lead on silver reacts directly with oxygen from the gas phase, but that a structure change in the lead overlayer at 0.5 ML coverage is causing the different oxidation behaviour at higher coverages.

9 Conclusions

It is clear that by preparing ultra thin overlayers of metal oxides on top of dissimilar metal substrates, the surfaces of these oxides becomes accessible to the modern surface science techniques. Problems with electrical charging, heat conductivity, sample mounting and cleanliness of the material can be circumvented. The oxides can be epitaxially grown and can be ordered by heating of the substrate. These oxide surfaces can be used as model systems for the study of high pressure chemical reactions. It is also possible to create new oxide materials with new properties. The properties depend on the combination of

metal oxide and substrate used. The oxidation state of the metal and the structure of the overlayer cannot always be varied at will. Judicious choice of the substrate metal, substrate orientation, the application of source material and the partial oxygen pressure during and after metal deposition is required to obtain the desired oxidation state and stoichiometry of the oxide. Similar preparation procedures might be useful in the production of clean and ordered films of other compounds and reactive materials such as carbides, nitrides, and halides.

Appendix I

The temperature at which the oxide is in thermodynamic equilibrium with an oxygen partial pressure of 1×10^{-9} Torr in table 1 for the reaction M_yO_x = yM + $\frac{x}{2}$ O_2 was calculated by means of the following relation:

$$\frac{x}{2}\ln(p_{O_2}) = -\frac{\Delta G^0_{f,298}}{298R} + \frac{\Delta H^0_{f,298}}{R}(\frac{1}{298} - \frac{1}{T}) \quad (1)$$

where p_{O_2} is the oxygen partial pressure in atmospheres, T is the temperature, x is the oxygen content of the oxide, R is the gas constant and $\Delta G^0_{f,298}$ and $\Delta H^0_{f,298}$ are the Gibbs free energy and enthalpy of formation of the oxide at 298 K respectively. The values for the oxides were obtained from reference [53]. The assumption is made that $\Delta H^0_{f,298}$ does not depend on the temperature. The different crystalline or amorphous phases of an oxide are all in equilibrium with 1×10^{-9} Torr within 10 K of the listed temperature.

References

[1] I.L. Sokol'skaya and S.A. Shakirova. *Sov. Phys. Solid State* **13** (1971) 262.

[2] S.A. Shakirova and I.L. Sokol'skaya. *Sov. Phys. Solid State* **13** (1971) 1441.

[3] R. Vanselow, J.P. Ross, and M. Gara. *J. Cryst. Growth* **23** (1974) 1.

[4] R. Vanselow. *Appl. Phys.* **2** (1973) 229.

[5] N.V. Mileshkina and A.K. Kaliteevskii. *Sov. Phys. Solid State* **11** (1970) 1456.

[6] J.P. Ross and R. Vanselow. *Appl. Phys.* **4** (1974) 161.

[7] Th. Beach and R. Vanselow. *Appl. Phys.* **4** (1974) 265.

[8] Y-B. Zhao and Y-W. Chung. *J. Catal.* **106** (1987) 369.

[9] A. Bukaluk, R. Siuda, M. Rozwadowski, and W. Bala. *Surf. Sci.* **171** (1986) L483.

[10] C.T. Campbell, K.A. Daube, and J.M. White. *Surf. Sci.* **182** (1987) 458.

[11] G. Pankov and M. Drechsler. *Zeit. Phys. Chem. NF* **31** (1962) 288.

[12] M.E. Levin, M. Salmeron, A.T. Bell, and G.A. Somorjai. *J. Chem. Soc., Faraday Trans. 1* **83** (1987) 2061.

[13] M.E. Levin, M. Salmeron, A.T. Bell, and G.A. Somorjai. *Surf. Sci.* **195** (1988) 429.

[14] M.E. Levin, K.J. Williams, M. Salmeron, A.T. Bell, and G.A. Somorjai. *Surf. Sci.* **195** (1988) 341.

[15] S.R. Bare, D.R. Strongin, and G.A. Somorjai. *J. Phys. Chem.* **90** (1986) 4726.

[16] D.R. Strongin, S.R. Bare, and G.A. Somorjai. *J. Catal.* **103** (1987) 289.

[17] D.R. Strongin and G.A. Somorjai. *Catal. Lett.* **1** (1988) 61.

[18] C.S. Ko and R.J. Gorte. *Surf. Sci.* **155** (1985) 296.

[19] R.A. Demmin, C.S. Ko, and R.J. Gorte. *ACS Symposium Series*, chapter Support Effects Studied on Model Supported Catalysts. Volume No. 298, 1986.

[20] R.A. Demmin and R.J. Gorte. *J. Catal.* **98** (1986) 577.

[21] U. Bardi, P.N. Ross, and G.A. Somorjai. *J. Vac. Sci. Technol.* **A 2** (1984) 40.

[22] U. Bardi and P.N. Ross. *Modifications of the surface properties of metals by oxide overlayers: I. oxidized zirconium deposited on the Pt(100) single crystal surface.* Technical Report, LBL-21772, 1986.

[23] R.A. Demmin and R.J. Gorte. *J. Catal.* **105** (1987) 373.

[24] C.S. Ko and R.J. Gorte. *J. Catal.* **90** (1984) 59.

[25] R.A. Demmin, C.S. Ko, and R.J. Gorte. *J. Phys. Chem.* **89** (1985) 1151.

[26] D.J. Dwyer, S.D. Cameron, and J. Gland. *Surf. Sci.* **159** (1985) 430.

[27] C.S. Ko and R.J. Gorte. *Surf. Sci.* **161** (1985) 597.

[28] R.J. Gorte, E. Altman, G.R. Corallo, M.R. Davidson, D.A. Ashbury, and G.B. Hoflund. *Surf. Sci.* **188** (1987) 327.

[29] C.M. Greenlief, J.M. White, C.S. Ko, and R.J. Gorte. *J. Phys. Chem.* **89** (1985) 5025.

[30] M.E. Levin, M. Salmeron, A.T. Bell, and G.A. Somorjai. *J. Catal.* **106** (1987) 401.

[31] M.E. Levin, M. Salmeron, A.T. Bell, and G.A. Somorjai. *Surf. Sci.* **169** (1986) 123.

[32] J.P.S. Badyal, A.J. Gellman, R.W. Judd, and R.M. Lambert. *Catal. Lett.* **1** (1988) 41.

[33] D. Chadwick, A.B. Christie, and M.A. Karolewski. *Vacuum* **31** (1981) 705.

[34] D. Chadwick and M.A. Karolewski. *Appl. Surf. Sci.* **9** (1981) 98.

[35] D. Chadwick and A.B. Christie. *Surf. Sci.* **82** (1979) L293.

[36] D. Chadwick and A.B. Christie. *ECOSS-3 Proc., Le Vide, les Couches Minces* **201** (1980) 407.

[37] C. Ocal, E. Martinez, and S. Ferrer. *Surf. Sci.* **136** (1984) 571.

[38] G.H. Vurens, M. Salmeron, and G.A. Somorjai. *Surf. Sci.* **201** (1988) 129.

[39] Y-W. Chung, G. Xiong, and C-C. Kao. *J. Catal.* **85** (1984) 237.

[40] R.M. Nix, R.W Judd, and R.M. Lambert. *Surf. Sci.* **205** (1988) 59.

[41] S.H. Overbury, P.A. Bertrand, and G.A. Somorjai. *Chem. Rev.* **75** (1975) 547.

[42] N.D. Shinn and P.J. Berlowitz. *J. Vac. Sci. Technol. A* **6** (1988) 597.

[43] R.W. Vook. *Intern. Metals Rev.* **27** (1982) 209.

[44] F.C.M.J.M. van Delft, A.D. van Langeveld, and B.E. Nieuwenhuys. *Thin Solid Films* **123** (1985) 333.

[45] K.J. Williams, M. Salmeron, A.T. Bell, and G.A. Somorjai. *Surf. Sci.* **204** (1988) L745.

[46] G.B. Raupp and J.A. Dumesic. *J. Catal.* **95** (1985) 587.

[47] G.B. Raupp and J.A. Dumesic. *J. Phys. Chem.* **88** (1984) 660.

[48] V.N. Erenenko, Yu. V. Naidikh, and A.A. Nosonovitch. *Zh. Fiz. Khim.* **34** (1960) 1018.

[49] F.H. Buttner, E.R. Funk, and H. Udin. *J. Phys. Chem.* **56** (1952) 657.

[50] R.G. Aldrich and D.V. Keller Jr. *J. Phys. Chem.* **72** (1968) 1092.

[51] M.A. van Hove and S.Y. Tong. *Surface Crystallography by LEED.* Springer Verlag, 1979.

[52] J.P. Biberian and G.A. Somorjai. *J. Vac. Sci. Technol.* **16** (1979) 2073.

[53] R.C. Weast (Ed.). *Handbook of Chemistry and Physics* 64^{th} *Ed.* CRC press, 1983.

[54] W.T. Tysoe, F. Zaera, and G.A. Somorjai. *Surf. Sci.* **200** (1988) 1.

Figure Captions

Figure 1. Schematic representation of the preparation of metal oxide overlayers on metal substrates.

Figure 2. (a) AES uptake curve of a lead overlayer on copper. A clear break is visible. (Reproduced with permission). (b) AES uptake curve for iron oxide on platinum. In general the break in AES uptake curves is hard to detect, without the help of additional techniques.

Oxide	T (K) for $p_{O_2}=10^{-9}$ Torr	Oxide	T (K) for $p_{O_2}=10^{-9}$ Torr
Al_2O_3	2561	Nd_2O_3	2855
Sb_2O_4	1094	NiO	1154
Sb_2O_5	928	NbO	1980
As_2O_5	884	NbO_2	1922
BeO	2876	Nb_2O_5	1869
Bi_2O_3	941	OsO_4	525
B_2O_3	2125	P_4O_{10}	1423
CdO	1210	KO_2	750
CaO	2915	K_2O_2	1076
CeO_2	2562	Sm_2O_3	2860
Ce_2O_3	2793	Sc_2O_3	2977
Cs_2O	1441	SiO_2	2227
Cr_2O_3	1853	Ag_2O	172
Eu_2O_3	2508	AgO_2	60
Eu_3O_4	2552	NaO_2	708
Ga_2O_3	1686	Na_2O	1699
Co_3O	1231	Na_2O_2	1163
Co_3O_4	1051	SrO	2756
CuO	762	SO_3	724
Cu_2O	890	Ta_2O_5	2005
Dy_2O_3	2872	TeO_2	801
Er_2O_3	2964	Tl_2O	816
GeO	1333	ThO_2	2915
GeO_2	1349	Tm_2O_3	2874
HfO_2	2745	SnO	1357
Ho_2O_3	2931	SnO_2	1343
In_2O_3	1402	TiO	2644
FeO	1476	TiO_2	2283
Fe_2O_3	1337	Ti_2O_3	2407
Fe_3O_4	1398	WO_2	1422
La_2O_3	2820	WO_3	1392
PbO	1032	UO_2	2674
PbO_2	647	UO_3	2030
Pb_3O_4	847	U_3O_7	2428
Li_2O	2523	U_3O_8	2237
Lu_2O_3	2934	VO	2092
MgO	2708	V_2O_3	2005
MnO	2043	V_2O_4	1741
MnO_2	1264	V_2O_5	1538
Mn_2O_3	1592	V_3O_5	2010
Mn_3O_4	1722	V_4O_7	1867
HgO	409	Yb_2O_3	2853
MoO_2	1419	Y_2O_3	2983
MoO_3	1242	ZnO	1626
		ZrO_2	2613

Table 1:

System	Growth Mode	Stoichiometry	Techniques	Reference
TiO_x/Pt	1 ML 2D	TiO_2/Ti^{4+}	AES,TPD	[11-19]
		anneal: TiO/Ti^{3+}	XPS,ISS	
TiO_x/Rh	1 ML: 2D >1 ML: 3D	TiO_2/Ti^{4+}	AES,TPD	[15,20-22]
		anneal: TiO/Ti^{3+}		[19, 13, 14]
TiO_x/Rh(111)	1 ML: 2D >1 ML: 2D		AES,TPD,ISS	[45]
TiO_x/Ni	1 ML: 2D		AES,TPD,XPS	[46, 47]
TiO_x/Ni(111)		x=1.0-1.5	AES,XPS	[39]
TiO_x/Pd	1 ML: 2D	anneal: TiO	AES,TPD	[27, 19]
TiO_x/Au		TiO_2/Ti^{4+}	AES,XPS	[13]
TiO_x/Ru(0001)	1 ML: 2D >1 ML:2D	TiO_2	AES,TPD,XPS	[32]
		anneal: TiO	LEED	
AlO_x/W		x<1.5	FEM	[3,5,6,30]
AlO_x/W(112)		x<1.5	FEM	[3, 4]
AlO_x/Rh	1 ML: 2D >1 ML: 3D	Al_2O_3	AES,TPD,XPS	[22-24]
AlO_x/Fe(111)	3D	Al_2O_3	AES,TPD,LEED	[31-33]
AlO_x/Fe(110)	3D	Al_2O_3	AES,TPD,LEED	[31-33]
AlO_x/Fe(100)	3D	Al_2O_3	AES,TPD,LEED	[31-33]
AlO_x/Re		x<1.5	FEM	[7]
AlO_x/Pt	3D	Al_2O_3	AES,TPD	[18]
AlO_x/Ni	3D		TPD,XPS	[46]
PbO_x/Cu		PbO	AES,XPS,UPS	[34-36]
PbO_x/Cu(111)		PbO	AES,XPS,UPS	[35-37]
PbO_x/Cu(210)		PbO	XPS,UPS	[36]
PbO_x/Ag		PbO	AES,XPS,UPS	[33, 34]
SiO_x/Re		SiO	FEM	[2]
SiO_x/W	1 ML: 2D >1 ML: 3D	SiO	FEM	[1]
SiO_x/Pt	3D	SiO/SiO_2	AES,TPD	[18]
ZnO_x/Au	1 ML: 2D >1 ML: 2D		AES	[54]
ZnO_x/Cu(111)		ZnO	AES,XPS,ISS,LEED	[10]
NbO_x/Pt	1 ML: 2D	Nb_2O_5	AES,TPD	[18, 19, 20]
ZrO_x/Pt(100)	1 ML: 2D >1 ML: 2D	ZrO_2	AES,TPD,LEED	[21, 22]
CrO_x/W(110)		(Cr_2O_3)	AES,TPD,LEED	[42]
FeO_x/Pt(111)	1 ML: 2D > 1ML: 2D	FeO	AES,XPS,ISS	[38]
			LEED,TPD	
MnO_x/Ni(111)	1ML: 2D	x=0.2-0.5	AES,TPD,HREELS	[8]
ReO_x/Pt		ReO,ReO_2,Re_2O_7	XPS	[54]
NdO_x/Cu(100)		0<x<1.5	AES,XPS,UPS,LEED	[40]

Table 2:

Schematic Representation of the Formation of ordered Metal Oxide Overlayers

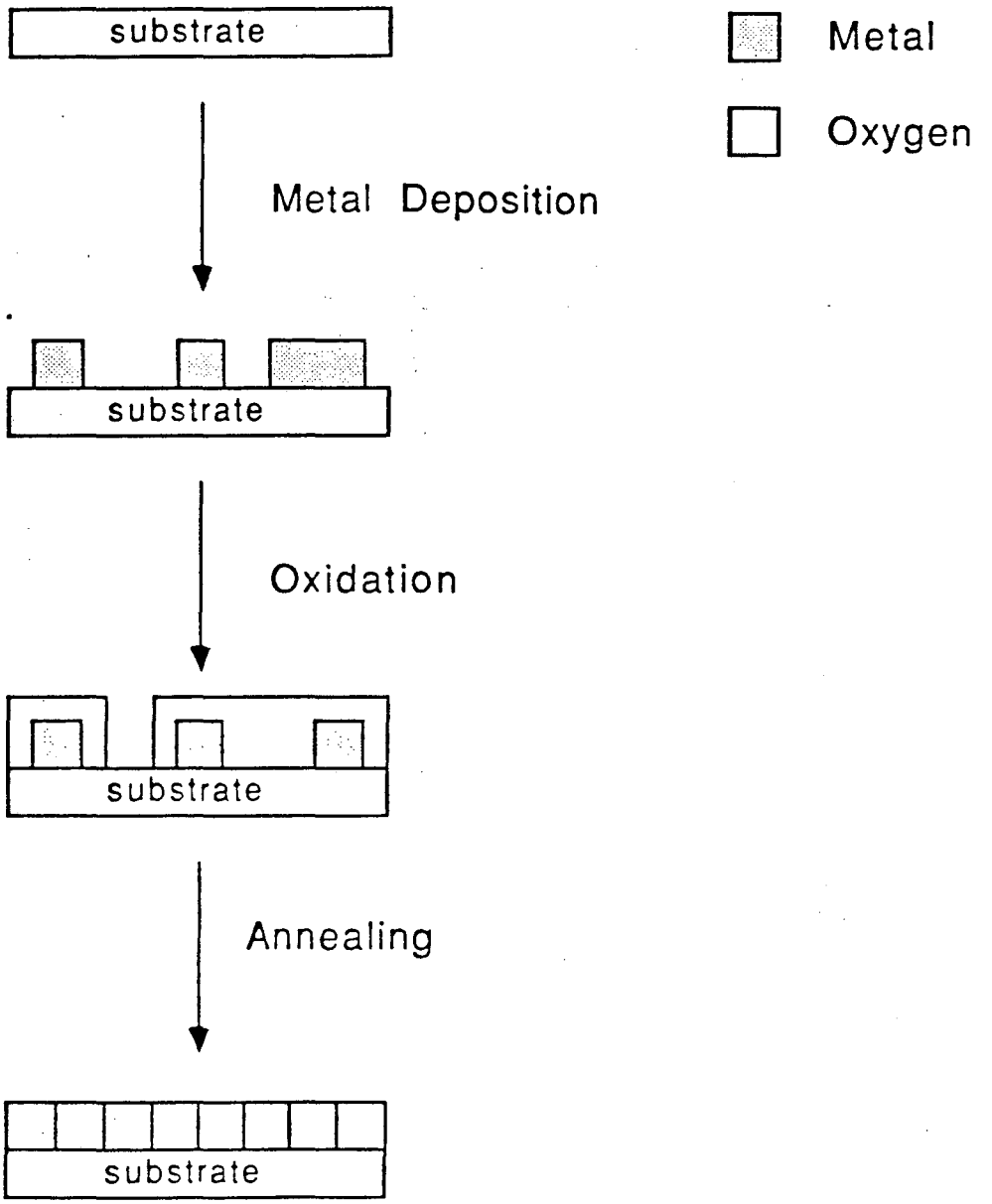

Fig. 1

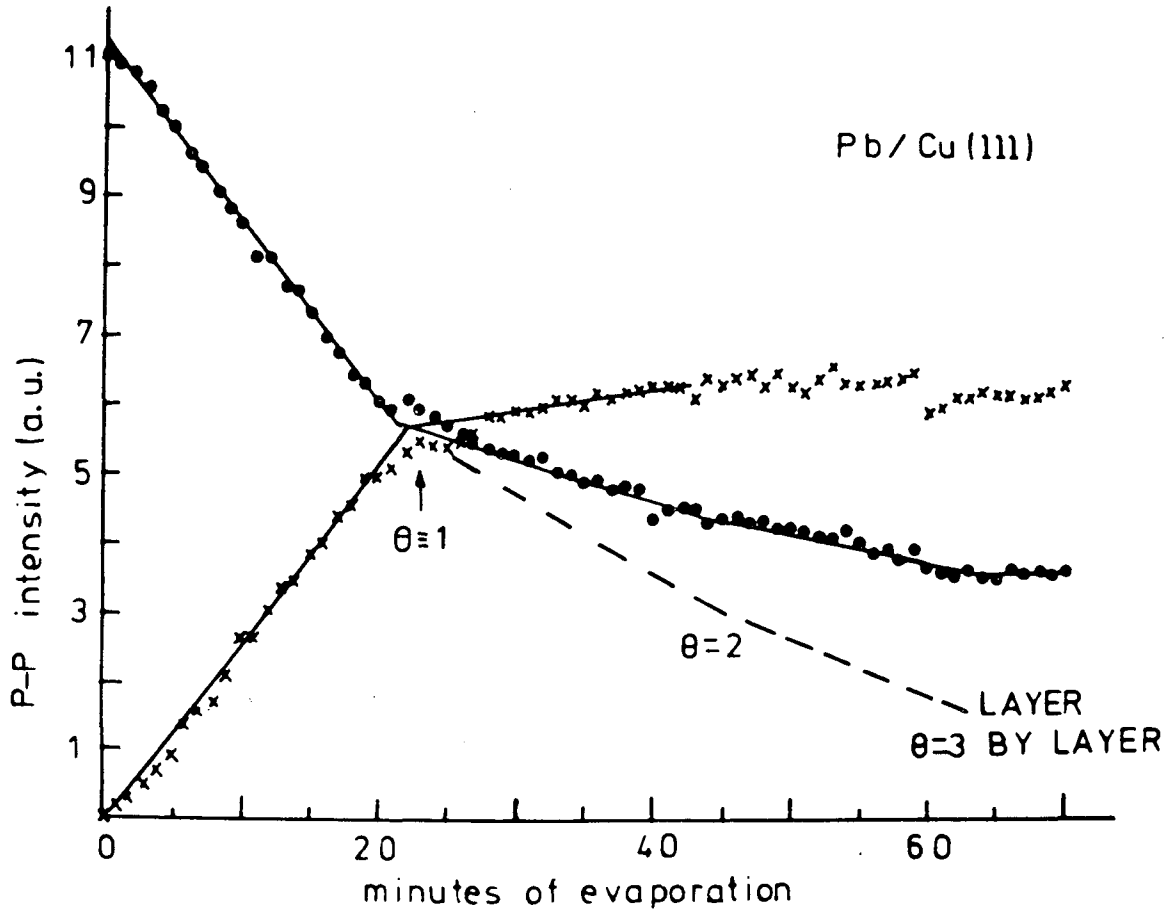
Pb / Cu (111)
P–P intensity (a.u.)
11
9
7
5
3
1
θ≡1
θ=2
LAYER
θ=3 BY LAYER
0
20
40
60
minutes of evaporation

Fig. 2A

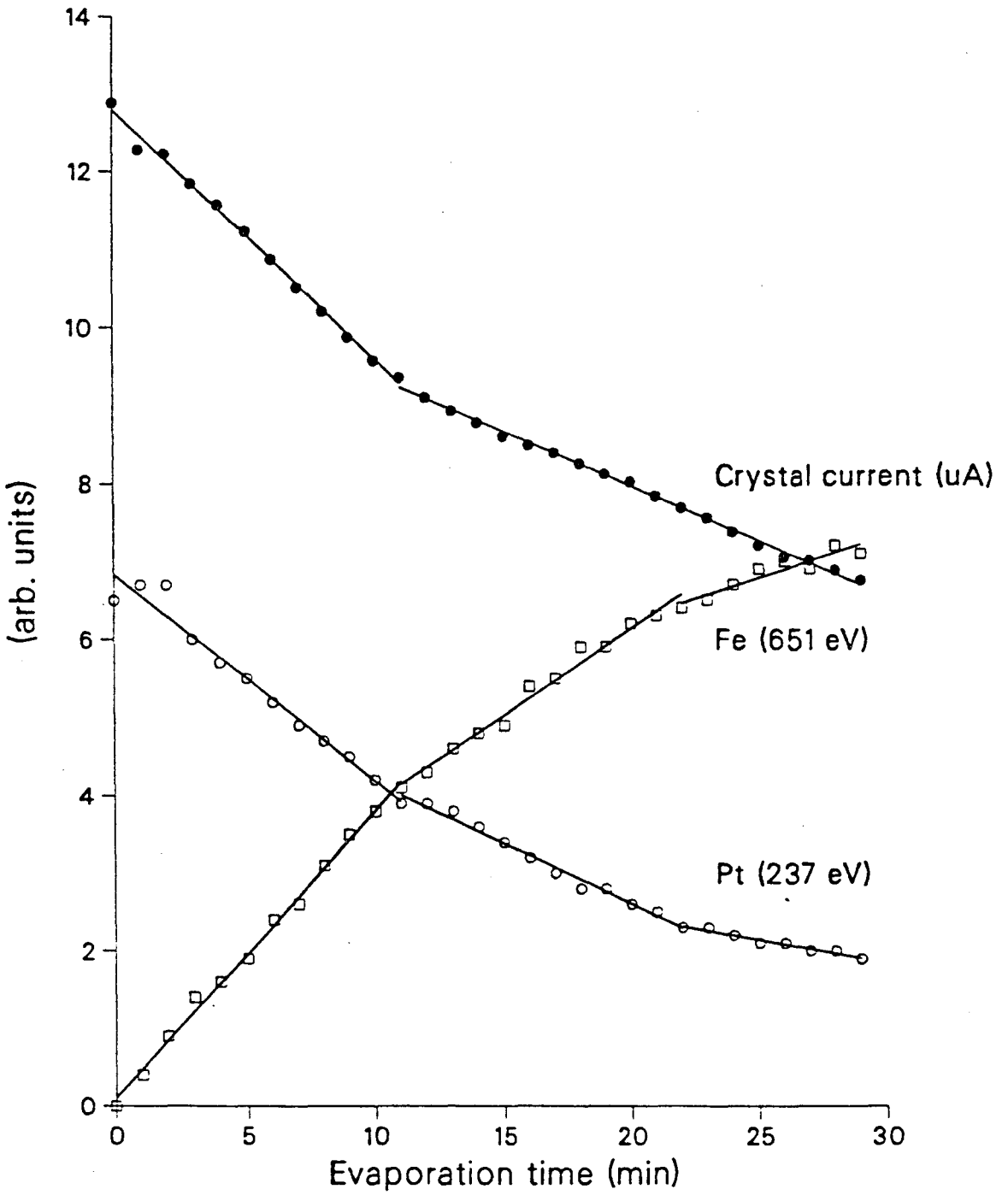
14
12
10
8
6
4
2
0
(arb. units)
0
5
10
15
20
25
30
Evaporation time (min)
Crystal current (uA)
Fe (651 eV)
Pt (237 eV)

Fig. 2B

LAWRENCE BERKELEY LABORATORY
CENTER FOR ADVANCED MATERIALS
1 CYCLOTRON ROAD
BERKELEY, CALIFORNIA 94720